IEEE Access
Multidisciplinary | Rapid Review | Open Access Journal

Received May 30, 2019, accepted June 22, 2019, date of publication July 3, 2019, date of current version July 23, 2019.

Digital Object Identifier 10.1109/ACCESS.2019.2926520

Adaptive Self-Deferral for Carrier Aggregation of LTE-LAA With RF Power Leakage in Unlicensed Spectrum

LONG HOANG VU AND JI-HOON YUN

Department of Electrical and Information Engineering, Research Center for Electrical and Information Technology, Seoul National University of Science and Technology, Seoul 01811, South Korea

Corresponding author: Ji-Hoon Yun (jhyun@seoultech.ac.kr)

This work was supported in part by the Institute for Information and Communications Technology Promotion (IITP) Grant funded by the Korea Government (MSIT) under Grant 2018-0-00828 and in part by the Basic Science Research Program through the National Research Foundation of Korea (NRF) funded by the Ministry of Education under Grant 2019R1A6A1A03032119.

ABSTRACT The licensed assisted access (LAA) is the new feature of 3GPP long-term evolution (LTE) that uses unlicensed spectrum as an additional bandwidth to meet ever-increasing mobile traffic demands. For fair coexistence with other incumbent systems such as Wi-Fi, LAA specifies the listen-before-talk (LBT) mechanism for channel access. LBT of LAA is also designed to support multi-carrier operation, which is the key to capacity increase, but inherent RF power leakage to adjacent carriers ruins the multi-carrier LBT and deteriorates aggregation capacity considerably. Self-deferral is a solution to solve this problem by aligning carriers' transmission times via transmission deferring of each carrier after backoff, for which the key to success is to find how long self-deferral must be. In this paper, we propose an algorithm to adjust a self-deferral period of the multi-carrier LBT adaptively to carrier loads for enhanced carrier aggregation capacity under RF power leakage. We formulate the target problem as an optimization problem whose objective is to maximize the expected number of aggregated carriers derived as a function of the self-deferral period and carrier loads. Then, we derive the optimum of the aggregation capacity maximization problem for the case of homogeneous interference patterns between carriers in a closed form. Due to the computational complexity of finding the global optimum for the general case of realistic heterogeneous interference patterns between carriers, we develop a suboptimal algorithm to configure the self-deferral period. Through extensive simulation, we demonstrate that the proper configuration of the self-deferral period is of importance and the proposed algorithm outperforms various LBT options in a wide range of network configuration by up to 72% in a single-spot scenario and 47% in 3GPP's indoor deployment scenario, while meeting fair coexistence with the Wi-Fi systems.

INDEX TERMS LTE-LAA, unlicensed spectrum, listen before talk, carrier aggregation, self-deferral, coexistence.

I. INTRODUCTION

The recent study of the 3rd generation partnership project (3GPP) has enabled the operation of LTE systems in unlicensed spectrum (e.g. 5 GHz band) [1]. This new feature, named *licensed assisted access* (LAA), is implemented as an extension of carrier aggregation such that a user equipment (UE) can establish a data channel with a cell operating a frequency carrier of unlicensed spectrum while its primary control channel still remains in a cell of licensed spectrum. To address the coexistence of LAA and other incumbent systems such as Wi-Fi (IEEE 802.11 WLAN) in the unlicensed spectrum, LAA is equipped with the *listen-before-talk* (LBT) mechanism [2] that, before accessing a carrier medium, an LAA eNodeB (eNB) has to sense the idle medium for a randomly chosen amount of time via *clear channel assessment* (CCA), which is also known as a *backoff* procedure.

Multi-carrier aggregation is still the key to capacity increase in unlicensed spectrum, thus LBT of LAA is designed to support multi-carrier operation as well with two options named *Type A* and *Type B* [2]. LBT Type A runs

The associate editor coordinating the review of this manuscript and approving it for publication was Mubashir Husain Rehmani.

independent LBT (backoff) processes for individual carriers while Type B runs a single backoff process for a primary carrier only like Wi-Fi's wide-band operation. Therefore, LBT Type A determines access timing of individual carriers differently based on each's channel condition while LBT Type B determines it identical for all carriers solely depending on the condition of the primary carrier. Thus LBT Type A is expected to better exploit multiple carriers than Type B (as will also be shown in Section VI).

In LBT Type A, however, inherent *RF power leakage* to adjacent carriers may ruin CCA of an LAA eNB. Once eNB starts transmission on a carrier, it senses the leaked power of the transmission on other carriers due to proximity of transceivers and concludes these carriers busy despite no activity of other systems. According to the spectral mask requirement of 3GPP for eNB in unlicensed spectrum [3], an eNB's transmission in any carrier can make it sense all other carriers to be busy (detailed in Section III). This problem results in poor utilization of multiple carriers and deteriorates aggregation capacity considerably.

Self-deferral was proposed as a solution to solve the RF power leakage problem of LBT Type A [4]. If an LAA eNB finishes a backoff process for a carrier earlier than for others, it self-defers transmission in the carrier by a specified time point, thus avoiding RF power leakage by this point to the other carriers having ongoing backoff processes. Then, on that time point, the eNB performs CCA again for a short period in all the carriers under self-deferral (i.e., with completed backoff processes) and starts transmission simultaneously on those sensed idle. However, self-deferral does not always guarantee the availability of more carriers for transmission, which highly depends on the period to self-defer for. A non-optimal self-deferral period may result in a small number of carriers completing backoff processes at the end of self-deferral or an increase of the possibility that other nodes (of either LAA or Wi-Fi) have already occupied some or all carriers among those under self-deferral. Moreover, these are also affected by the load conditions of individual carriers.

In this paper, we propose an algorithm to adapt the self-deferral period for multi-carrier operation of LTE-LAA with LBT Type A, thus providing throughput improvement along with fair coexistence with incumbent Wi-Fi systems. We formulate the target problem as an optimization problem whose objective is to maximize the expected number of aggregated carriers derived as a function of the self-deferral period and carrier loads. We derive the optimum of the problem for the case of homogeneous interference patterns between carriers. Due to the computational complexity of finding the global optimum for the case of realistic heterogeneous interference patterns between carriers, we develop a suboptimal algorithm to configure the self-deferral period for the general case. The algorithm is designed to exploit the closed-form solution of the case of homogeneous interference patterns; it obtains the solution for the interference pattern of each carrier and picks the best one among all solutions in terms of the expected number of aggregated carriers. The algorithm is activated only when the status of carriers is changed enough to impact the choice of the self-deferral period so as to reduce computational overhead further.

For evaluation, we compare the performance of various LBT options under different RF power leakage cases in two network deployment scenarios where Wi-Fi systems coexist. Through extensive simulation work, we demonstrate that the proposed algorithm enhances system throughput considerably over other LBT options while meeting fair coexistence with Wi-Fi systems, e.g. the enhancement gain over no self-deferral is obtained as up to 72% in a single-spot scenario and 47% in 3GPP's indoor deployment scenario while a fixed self-deferral period achieves much lower performance than no self-deferral case.

In summary, the main contributions of our work are listed as follows:

- Derivation of the optimal period of self-deferral to maximize the expected number of aggregated carriers for the case of homogeneous interference patterns between carriers.
- Design of a low-complexity algorithm to determine a suboptimal self-deferral period for the case of heterogeneous interference patterns between carriers.
- Comprehensive simulation to show the performance gain of the proposed algorithm over various LBT options with coexistence of multiple operators and incumbent Wi-Fi systems.

The rest of the paper is organized as follows. In Section II, we review the related work on LTE-LAA and LBT mechanisms. Section III presents the background on multi-carrier operation of LTE-LAA and the RF power leakage problem. The system model under consideration is presented in Section IV. In Section V, we describe in detail the problem formulation, the solution for homogeneous interference patterns between carriers and the design of the proposed algorithm. In Section VI, we evaluate the proposed algorithm in comparison with various LBT options via simulation. Finally, Section VII concludes the paper.

II. RELATED WORK

A. CHANNEL ACCESS PROCEDURE

There are two major approaches for LTE's coexistence with other systems in unlicensed spectrum: (1) *duty-cycling* and (2) *listen-before-talk* (LBT).

Duty-cycling lets an LTE system transmit only during a periodic on period and mute otherwise so that other systems can use the channel medium during the mute (off) period. This approach is known as LTE-U [5] and does not require any modification of the current LTE specification [5]–[18]. Duty-cycling was designed mainly aiming for early deployment in the unlicensed spectrum bands where the use of LBT is not mandated by regulations, thus not as universal as the LBT approach.

Many countries have regulatory requirements mandating the use of LBT in unlicensed spectrum. Thus the channel access design of LTE-LAA is based on LBT so as to

be a universal framework for world-wide deployment [19]. There have been a number of research works on various LBT designs and schemes to adjust the contention window of LBT. In [20], a fixed sensing period of LBT as a fraction of time within a frame was proposed. A fixed contention window for LBT was proposed in [21]–[23]. Similarly, Mukherjee *et al.* [23] proposed an LBT procedure with a fixed CCA window and a freeze period to the next subframe boundary during which backoff is suspended. Various schemes to adjust the contention window of LBT were proposed in [24]–[30] as well. In particular, Tao *et al.* [29] proposed an LBT algorithm to achieve both channel access fairness and QoS by avoiding disordered adjustment and smoothing of the contention window. A fair downlink traffic management scheme was proposed in [28] which adjusts the minimum contention window based on traffic loads.

The impact of other LBT parameters was also studied and schemes to adjust them were proposed. Determining the energy detection (ED) threshold of LAA is also an important issue. It was demonstrated as a significant factor of coexistence in [25]–[27]. In particular, Xu *et al.* [26] showed that a proper ED threshold is necessary for fair coexistence of different systems. Li *et al.* [25] proposed to change the ED threshold of LAA adaptively per user and base station. Considering the different levels of CCA thresholds between LAA and Wi-Fi, Lee *et al.* [27] modeled the coexistence problem by a joint Markov chain. For channel occupancy time of LAA, Yoon *et al.* [31] proposed an adaptive adjustment scheme to guarantee both fair airtime and improved throughput of Wi-Fi. Yin *et al.* [30] proposed to adjust the population of LAA users, i.e., admission control, to minimize the contention window size and collision probability of Wi-Fi users.

B. RADIO RESOURCE COORDINATION

Another method of coexistence is based on resource coordination between LAA and Wi-Fi systems such as spectrum assignment and interference management. A cognitive coexistence scheme to achieve both spectral efficiency and fairness between LAA and Wi-Fi was presented in [18]. Sallent *et al.* [32] proposed a channel selection scheme using Q-learning set-up of an LTE-U carrier. Sagari *et al.* [33] applied a centralized optimization framework that is used to exchange information for dynamic spectrum management and inter-network coordination between LAA and Wi-Fi systems. To combat uncontrollable interference from coexisting Wi-Fi networks which may cause a hidden terminal problem, the authors in [34] developed a dynamic switching mechanism between scheduling-based access and random access for UL transmission of LAA. Tsinos *et al.* [35] extended the resource allocation problem to consider aggregation of licensed and unlicensed carriers with MIMO. Jointly optimizing channel assignment, sub-carrier assignment and power allocation between licensed and unlicensed bands was proposed in [36]. There have also been several attempts to analyze and solve the radio resource coordination problem based on game theory considering LAA and Wi-Fi devices as game players to win channel resources [15], [37]–[39].

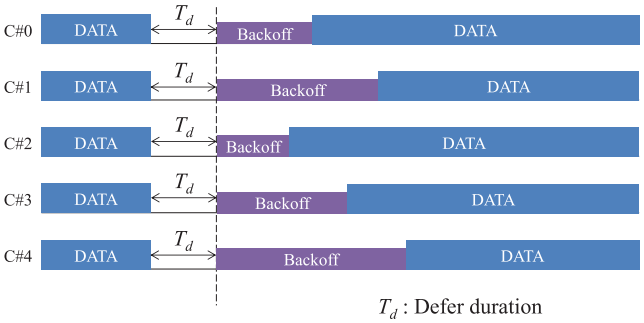

FIGURE 1. Multi-carrier LBT procedure: Type A (with no RF power leakage).

C. MULTI-CARRIER LISTEN-BEFORE-TALK MECHANISM

Multi-carrier LBT for LTE-LAA has been designed and the framework of self-deferral was discussed in 3GPP [4], [40]–[48]. However, most research works on LBT of LAA considered a single-carrier case. There have only been several studies on multi-carrier LBT. Liu and Shen [49] proposed a primary-carrier selection mechanism for LBT Type B that a carrier which completes a backoff process first is selected as a primary carrier. Wang *et al.* [50] studied the performance of LBT Type B, then proposed a mechanism to switch on and off multi-carrier aggregation based on traffic loads. Vu and Yun [51] proposed a new multi-carrier LBT mechanism as a hybrid of Type A and Type B; it divides carriers into several groups between which guard-band carriers are placed, thus letting multiple groups operate simultaneously. Carrier grouping and selection of a primary carrier in each group is made based on carrier loads. The work of this paper differs from [51] in that we optimize the operation of the present LBT framework of LTE-LAA rather than designing a new LBT mechanism.

III. BACKGROUND

In this section, we explain the LBT procedure of LAA for multi-carrier aggregation and the accompanied RF power leakage problem.

A. MULTI-CARRIER LBT PROCEDURE

There are two types of multi-carrier LBT in LAA: Type A and B [2]. The major difference between two types is the number of carriers for each of which an independent backoff process runs:

- Type A: an independent backoff process is run for each carrier;
- Type B: a backoff process is run for a single primary carrier only.

In LBT Type A, as illustrated in Fig. 1, eNB runs an independent backoff process for each carrier, thus can exploit individual carriers adaptively to each's condition. After a carrier is sensed idle via CCA for a defer duration of T_d, its

backoff count starts to decrease every slot time T_{sl}. When the backoff count of a carrier becomes zero, the eNB can start transmission in the carrier.

The other option, Type B, is designed similar with the wide-band channel access mechanism of Wi-Fi as illustrated in Fig. 2. With LBT Type B, eNB selects a primary carrier and runs a backoff process on this carrier only. On the other carriers called *secondary* carriers, a short CCA during T_{mc} is performed immediately before the backoff count of the primary carrier becomes zero. Then, transmission starts on the primary carrier and the secondary ones which are sensed idle via the short CCA. Unlike Wi-Fi, no channel bonding rule is applied in LAA.

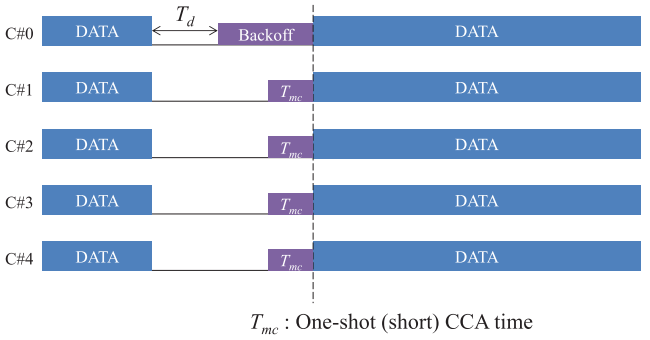

FIGURE 2. Multi-carrier LBT procedure: Type B.

B. RF POWER LEAKAGE PROBLEM

In the 3GPP Technical Specification 36.104 [3], the transmit spectral power mask of LTE-LAA for 20 MHz carrier bandwidth in 5 GHz unlicensed band is specified as shown in Fig. 3. Under the maximum allowable transmit power of 23 dBm at eNB, the restriction of maximum possible RF power leakage from an ongoing transmission to its adjacent carriers ranges from -27.6 (for the first adjacent (neighboring) carrier) to -40 dBm (for all beyond the 9th adjacent carrier). This level of RF power leakage is higher than the ED threshold of LAA ranging from -82 to -62 dBm. Thus, as illustrated in Fig. 4(a), once eNB starts a transmission on a carrier (C#2 in the figure) which finished its backoff first, the eNB may sense other carriers busy and freeze their backoff counts unnecessarily. This problem is called the *RF power leakage problem* [4], [40]–[48].

To combat the RF power leakage problem of LBT Type A, a solution called *self-deferral* (SD) was proposed [4]; the operation is illustrated in Fig. 4(b) and explained in the following. An LAA eNB defers transmissions until a specific time point called *LBT synchronization boundary* (LSB) for all carriers after finishing individual backoff processes so that transmissions on these carriers start at the same time, thus avoiding the RF power leakage problem between them. At LSB, eNB performs CCA for a short time interval T_{sl} on the carriers with zero backoff counts and starts transmission on those sensed idle. However, there is no guarantee to use more carriers at the end of self-deferral (i.e., more carriers

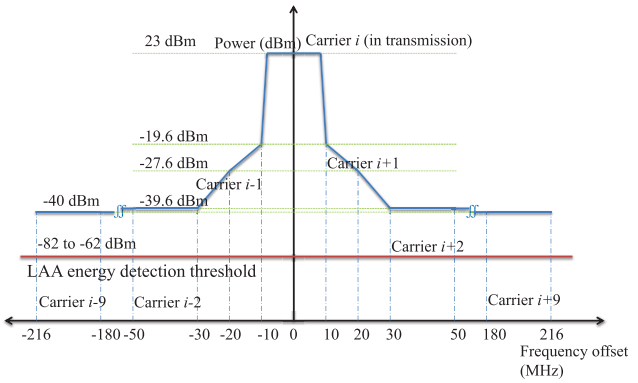

FIGURE 3. Spectral power mask of LTE-LAA for 20 MHz carrier bandwidth in 5 GHz band.

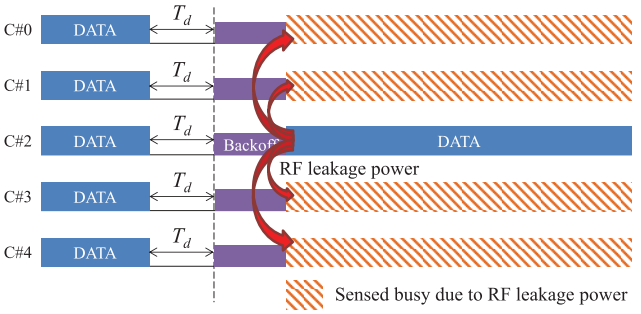

(a) LBT Type A with RF power leakage

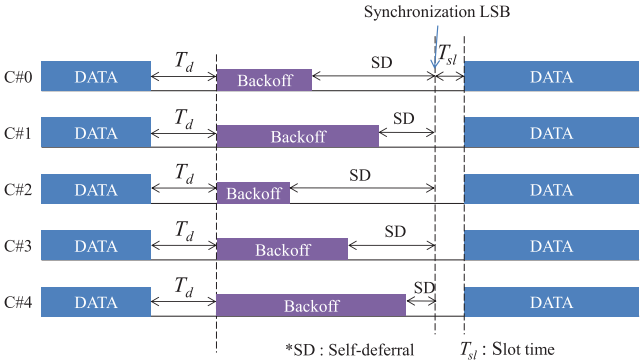

(b) LBT Type A with self-deferral (SD)

FIGURE 4. Illustration of the RF power leakage problem of LBT Type A and the self-deferral solution. (a) LBT Type A with RF power leakage. (a) LBT Type A with self-deferral (SD).

are sensed idle at LSB) than without SD (Fig. 1) due to other interference sources such as Wi-Fi devices and other LAA eNBs/UEs.

Another approach is to let an LAA eNB assume a carrier to be idle although it is sensed busy if the eNB is transmitting in another carrier. However, this does not guarantee that there exists no activity of other transmitters in the carrier, and moreover violates the regulations that force the use of LBT. Alternatively, canceling such a leaked RF signal (like the self-interference cancellation of full-duplex communication) can also be considered, but at the expense of additional hardware and processing overhead.

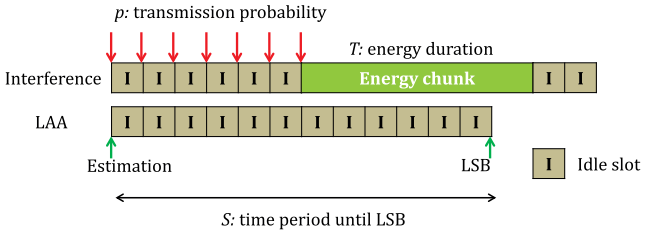

FIGURE 5. Illustration of the self-deferral model.

LBT Type B has no RF power leakage problem inherently. However, it may not be able to exploit each carrier more efficiently than Type A (as will be shown in Section VI) since it monitors (i.e., runs a backoff process in) a single primary carrier only. Therefore, selection of the primary carrier has a considerable impact on the performance of LBT Type B. If a selected one is busy, eNB does not exploit whole carriers well (even though secondary carriers are idle).

IV. SYSTEM MODEL

This section describes the network deployment model in unlicensed spectrum and the self-deferral model of LAA eNBs under consideration.

A. NETWORK MODEL

We consider an LTE-LAA network which is composed of multiple LAA eNBs and multiple UEs connected to each eNB. The frequency spectrum used by the LTE-LAA network is a set of consecutive 20 MHz carriers in unlicensed spectrum where Wi-Fi systems coexist. For data transmission, eNB performs either LBT Type A or B and transmits on up to N carriers at once according to an LBT result. eNB transmits downlink (DL) subframe(s)[1] first and then scheduled UEs transmit uplink (UL) subframe(s) immediately after the DL subframe. A UE performs a short CCA for 25 μs right before its frame transmission and transmits only on the carriers sensed idle. The coexisting Wi-Fi network contains multiple access points (APs) and connected user stations.

B. SELF-DEFERRAL MODEL

If an LAA eNB performs self-deferral with LBT Type A, the eNB runs individual backoff processes on different carriers, but sets an *LBT synchronization boundary* (LSB) at which the eNB starts transmissions over the carriers having zero backoff counts and sensed idle by the final short CCA. We make an extended definition of a *self-deferral period* denoted by S as the period of time from its estimation point until LSB. Thus, for some carrier, S may include remaining backoff time if the estimation of S is made before the backoff process of the carrier finishes. We express S in terms of the number of backoff slots. Fig. 5 illustrates the self-deferral model and the definition of S. We define $S_{\max}$ as the maximum allowable value of S to limit the waiting time for transmission.

[1] A subframe is 1 ms long.

We assume that each LAA eNB is equipped with Wi-Fi interface(s) as well and capable of measuring Wi-Fi loads in a carrier based on the detection of Wi-Fi preambles, as the CSAT (Carrier-Sensing Adaptive Transmission) technology of Qualcomm does [52]. Through CCA of the Wi-Fi interface in individual carriers, eNB collects the statistics of each carrier's Wi-Fi traffic load as two-tuple information: the probability for an energy chunk of Wi-Fi to start in a slot and the average duration of an energy chunk, which we denote by p_i and T_i, respectively, for carrier i. We need to determine S such that the total LAA aggregation capacity is maximized. It is noted that we consider Wi-Fi loads only in the estimation of a self-deferral period since a transmission burst of LAA typically spans multiple milliseconds due to subframe-basis transmission and following UL subframes of scheduled UEs. Therefore, deferring until a transmission burst of LAA finishes is not beneficial.

V. SELF-DEFERRAL ADAPTATION ALGORITHM

In this section, we present in detail the proposed adaptive self-deferral algorithm for multi-carrier LBT Type A.

A. PROBLEM FORMULATION

We formulate the target problem as the problem to determine an optimal self-deferral period such that the average number of aggregated carriers at once is maximized. Let $\mathcal{N}$ be the set of consecutive carriers that an LAA eNB can aggregate for data transmission and N be the number of carriers in $\mathcal{N}$. Carriers of $\mathcal{N}$ are indexed from 1 to N. We define P^i_{succ} as the probability that the LAA eNB transmits on carrier i successfully at the end of self-deferral. It is noted that, with the transmission time alignment of carriers by self-deferral, the LAA eNB's transmission on a carrier does not affect its transmission success probabilities on other carriers. Therefore, the average number of carriers to be aggregated after self-deferral is given as $\sum_{i\in\mathcal{N}} P^i_{succ}$. Thus the target problem P of the algorithm is formulated as

$$P : \max_{S} \sum_{i\in\mathcal{N}} P^i_{succ} \tag{1}$$

where P^i_{succ} is the function of S.

In what follows, we (1) derive the optimum of P in the case of homogeneous interference patterns between carriers first and (2) extend the solution to the general case with heterogeneous interference patterns next.

B. SOLUTION FOR HOMOGENEOUS INTERFERENCE PATTERNS BETWEEN CARRIERS

Since carriers have homogeneous interference patterns, we have $P^1_{succ} = \cdots = P^N_{succ}$. Thus we omit the super/subscript of carrier index i in this subsection. Then, we have

$$\sum_{i\in\mathcal{N}} P^i_{succ} = NP_{succ}. \tag{2}$$

That is, the problem P is reduced to maximization of P_{succ}.

During a self-deferral period of eNB, energy chunk(s) may appear in a carrier. Then, the condition that eNB succeeds to use the carrier after self-deferral is that all energy chunks have already ended before the end of self-deferral. We denote the successful carrier access probability of eNB when k energy chunks appear during S and end before LSB by $P_{succ,k}$. A successful access to a carrier with k energy chunks during S is made when S is composed of k slots having the beginning of an energy chunk, $k(T-1)$ slots having an ongoing energy chunk and the remaining $(S-kT)$ slots having no energy chunk. Thus $P_{succ,k}$ is obtained as

$$P_{succ,k} = \binom{S-k(T-1)}{k} p^k (1-p)^{S-kT}. \tag{3}$$

Therefore, if m is the maximum number of energy chunks that can appear during a self-deferral period, then we have the total successful channel access probability of eNB at the end of self-deferral as

$$P_{succ} = \sum_{k=0}^{m} P_{succ,k}. \tag{4}$$

As the self-deferral period S gets longer, an LAA eNB experiences longer waiting time before transmission. Thus we let no more than one energy chunk ($m=1$) during S be targeted in the following (extension to higher m is also possible). Then, (4) is rewritten as

$$\begin{aligned} P_{succ} &= (1-p)^S + \binom{S-T+1}{1} p(1-p)^{S-T} \\ &= (1-p)^S + (S-T+1)p(1-p)^{S-T}. \end{aligned} \tag{5}$$

Proposition 1: P_{succ} of (5) is the concave function of S for $S \le \hat{S}$ and the convex function for $S > \hat{S}$ where $\hat{S}$ is given as

$$\hat{S} = T - 1 - \frac{2}{\ln(1-p)} - \frac{(1-p)^T}{p}. \tag{6}$$

Proof: The first-order derivative of P_{succ} with respect to S is obtained as

$$\begin{aligned} \frac{\partial P_{succ}}{\partial S} &= (1-p)^S \ln(1-p) + p(1-p)^{S-T} \\ &\quad + (S-T+1)p(1-p)^{S-T}\ln(1-p) \\ &= (1-p)^S \left[\ln(1-p) + \frac{p}{(1-p)^T} \right. \\ &\quad \left. + \frac{(S-T+1)p\ln(1-p)}{(1-p)^T} \right] \\ &:= (1-p)^S f(S) \end{aligned} \tag{7}$$

and the second-order derivative is obtained as

$$\begin{aligned} &\frac{\partial^2 P_{succ}}{\partial S^2} \\ &= (1-p)^S \ln^2(1-p) + 2p(1-p)^{S-T}\ln(1-p) \\ &\quad + (S-T+1)p(1-p)^{S-T}\ln^2(1-p) \\ &= (1-p)^S \ln(1-p)\left[f(S) + \frac{p}{(1-p)^T} \right]. \end{aligned} \tag{8}$$

Note that $f(S)$ is a monotonically decreasing (linear) function of S since $\ln(1-p)$ is negative ($0 < p < 1$). Then, the sign of $\frac{\partial^2 P_{succ}}{\partial S^2}$ is non-positive, i.e., P_{succ} is concave, if $f(S) + \frac{p}{(1-p)^T} \ge 0$ which leads to $S \le \hat{S}$ as given in (6). In the same manner, $\frac{\partial^2 P_{succ}}{\partial S^2}$ is positive (P_{succ} is convex) if $S > \hat{S}$. □

According to Proposition 1, the optimum of P is obtained as follows.

Proposition 2: The optimal S maximizing P_{succ} is obtained as

$$S^* = \arg \max_{S \in \{S', S_{\max}\}} P_{succ} \tag{9}$$

where

$$S' = T - 1 - \frac{1}{\ln(1-p)} - \frac{(1-p)^T}{p}. \tag{10}$$

Proof: For $S \le \hat{S}$, P is a concave maximization problem and thus any points that satisfy the Karush-Kuhn-Tucker (KKT) conditions are optimal [53]. Exploiting one of the conditions, $\frac{\partial P_{succ}}{\partial S} = 0$, we obtain the optimal S in this range as S' of (10). For $\hat{S} < S \le S_{\max}$, P_{succ} is a convex function and maximized at a boundary point, i.e., $S_{\max}$. Finally, the optimal S in the whole range is picked among the two points. □

Fig. 6 illustrates how the pattern of carrier load (represented by p and T) impacts S^*. First, as p increases, S^* decreases. This is because high p means a crowded carrier and an LAA eNB should use a shorter self-deferral period for better contending with other devices; otherwise, it is more probable for other devices to occupy the carrier during self-deferral. Second, S^* increases as T increases. This is because an LAA eNB has to wait longer to see idle medium once it is occupied.

Fig. 7 shows the gap $\hat{S} - S'$ that is derived as $-\frac{1}{\ln(1-p)}$ in the concavity range of P_{succ}. As shown in the figure, the gap is always positive, implying that the optimum in the concavity range is not on the boundaries of the range.

C. LOW-COMPLEXITY ALGORITHM FOR HETEROGENEOUS INTERFERENCE PATTERNS BETWEEN CARRIERS

We now consider the general case that carriers have heterogeneous interference patterns, i.e., individual p_i and T_i, which is closer to practical conditions. Extending Proposition 1 to this case, however, is not straightforward; we obtain different $\hat{S}$ of P^i_{succ} for each i, thus their sum in (1) leads to a number of distinct ranges within each of which the sum of concave and convex functions differs. Then, we have to find an optimizer of the sum within each range. Therefore, extending the previous approach for the general case is not tractable. P is a non-convex non-linear optimization problem for which finding the global optimizer is computationally inefficient in general.

In order to combat this challenge, we design an algorithm to find a suboptimal solution of a self-deferral period. The design approaches to achieve low computational complexity are as follows:

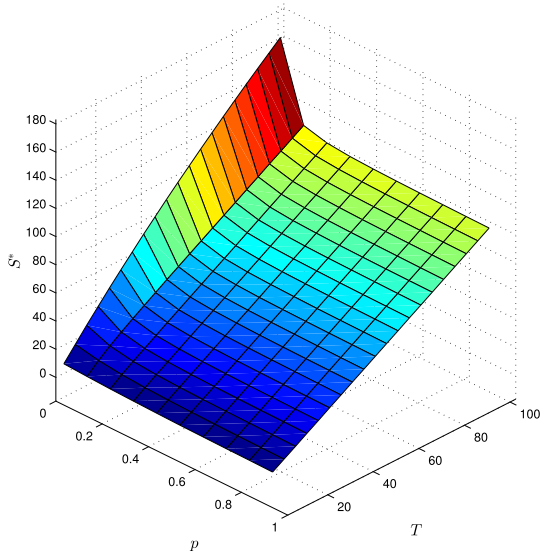

FIGURE 6. Optimal S for varying p and T in the case of homogeneous interference patterns between carriers.

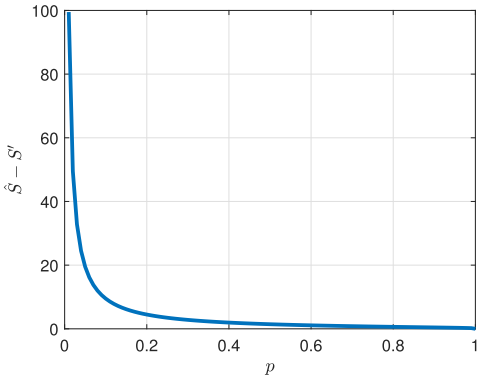

FIGURE 7. Gap between $\hat{S}$ and S'.

- Event-driven estimation triggering: Instead of finding a solution continuously over time, the estimation of a self-deferral period is triggered by a specific event that implies a significant change of a carrier's status;
- Suboptimal solution finding: Instead of finding the global optimizer, the algorithm finds suboptimal solutions exploiting the result of the previous subsection, picks the best and keeps updating it whenever the estimation of a self-deferral period is triggered.

In what follows, we detail the algorithm design.

First, the algorithm tracks the state of each carrier as shown in Fig. 8 and triggers self-deferral period estimation when a carrier transits to a specific state. At any time, a carrier is classified into one of the following three states and P^i_{succ} is obtained depending on the state:

- *BO-IDLE*: Carrier i is sensed idle during backoff. P^i_{succ} is obtained similar with (3) and (4) as

$$P^i_{succ} = \sum_{k=0}^{m} \binom{S - k(T_i - 1)}{k} p_i^k (1 - p_i)^{S - kT_i}. \quad (11)$$

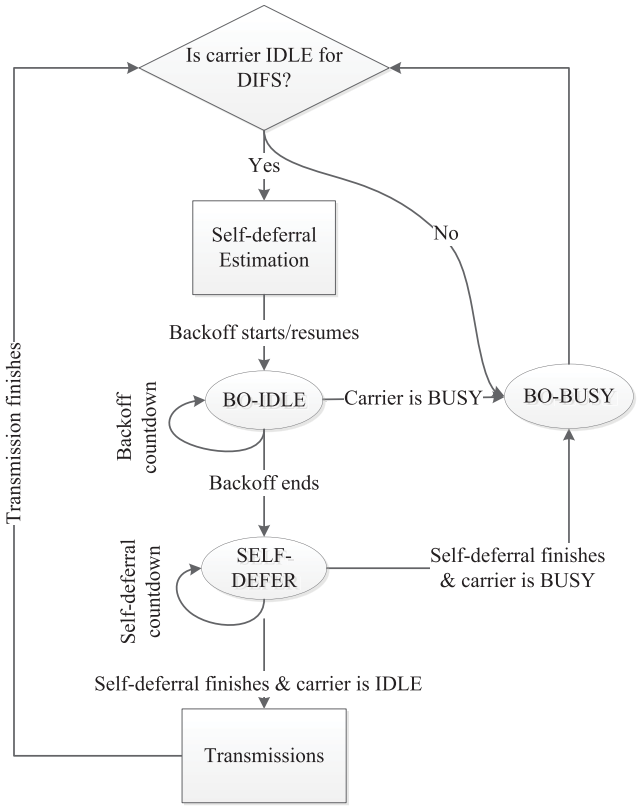

FIGURE 8. State transition diagram of a carrier in the proposed algorithm.

- *BO-BUSY*: Carrier i is sensed busy during backoff. We do not include a carrier in this state for determination of a self-deferral period. This is because self-deferral does not start for a carrier unless its state transits to BO-IDLE first.
- *SELF-DEFER*: The eNB is performing self-deferral for this carrier. When period estimation is triggered, if carrier i is already in SELF-DEFER starting t_{sd} earlier, we obtain P^i_{succ} as the sum of the probabilities that k energy chunks appear during the total self-deferral period $t_{sd} + S$ for $0 \le k \le m$, and write it as

$$P^i_{succ} = \sum_{k=0}^{m} \binom{t_{sd} + S - k(T_i - 1)}{k} p_i^k (1 - p_i)^{t_{sd} + S - kT_i}. \quad (12)$$

That is, the algorithm triggers self-deferral period estimation if a carrier changes its state to BO-IDLE, expecting that a significant change of the carrier's status has been made and a better choice of a self-deferral period could be produced from it. The pseudo code of the estimation is given in Algorithm 1. The estimation includes all carriers in either BO-IDLE or SELF-DEFER to update their optimal values as well. We let the sets of BO-IDLE and SELF-DEFER carriers be denoted by $\mathcal{N}_{idle}$ and $\mathcal{N}_{sd}$, respectively.

When self-deferral period estimation is triggered, the algorithm calculates a self-deferral period value for each of carriers in $\mathcal{N}_{idle} \cup \mathcal{N}_{sd}$ according to (9) assuming that

Algorithm 1 Self-Deferral Period Estimation

S: Self-deferral period
Initialize $\hat{P}^{+}_{succ} = 0$
for all $i \in \mathcal{N}_{idle} \cup \mathcal{N}_{sd}$ **do**
  Find S^* from (9) with $p = p_i$ and $T = T_i$
  Initialize $P^{+}_{succ} = 0$
  for all $j \in \mathcal{N}_{idle} \cup \mathcal{N}_{sd}$ and $i \neq j$ **do**
    if $j \in \mathcal{N}_{idle}$ **then**
      Calculate $P^{j}_{succ}(S^*)$ according to (11)
    else if $j \in \mathcal{N}_{sd}$ **then**
      Calculate $P^{j}_{succ}(S^*)$ according to (12)
    end if
    $P^{+}_{succ} \leftarrow P^{+}_{succ} + P^{j}_{succ}(S^*)$
  end for
  if $P^{+}_{succ} > \hat{P}^{+}_{succ}$ **then**
    $\hat{S}^* \leftarrow S^*$
    $\hat{P}^{+}_{succ} \leftarrow P^{+}_{succ}$
  end if
end for

TABLE 1. Simulation parameters.

Parameter	LAA	Wi-Fi
Frequency	5 GHz	
Carrier bandwidth	20 MHz	
Number of carriers	4	
RF power leakage bandwidth	[0, 20, 40, 60] MHz	
Tx power	18 dBm for both eNB/AP and user device	
Slot time T_{sl}	9 μs	
Defer duration T_d and DIFS	34 μs	
Short CCA time T_{mc} and PIFS	25 μs	
$CW_{\min}$	16	
$CW_{\max}$	1024	
MCS	QPSK, 16QAM, 64QAM	802.11ac's MCSs except 256QAM
Energy detection threshold	-72 dBm	-62 dBm
Preamble detection threshold	N/A	-82 dBm
Link adaptation	Channel state information-based	

interference patterns of all the other carriers are identical to the chosen carrier. Then, if this value improves the total objective $\sum_{i \in \mathcal{N}_{idle} \cup \mathcal{N}_{sd}} P^{i}_{succ}$, the algorithm updates the final self-deferral period with it; otherwise, it keeps the old one. Finally, the algorithm applies the self-deferral period that achieves the maximum total objective among the ones considered so far.

VI. PERFORMANCE EVALUATION

In this section, we perform performance evaluation in coexistence scenarios of LTE-LAA and Wi-Fi networks with various LBT options. For comparison, the considered options of LBT Type A for LAA are no self-deferral (NoSD), self-deferral using a fixed period (FixedSD), adaptive self-deferral using the period determined by the proposed algorithm, denoted by *AdaSD*, and the one using the optimal period found by the Nelder-Mead numerical method [54] of the Microsoft Solver Foundation (MSF) library [55], denoted by *OptSD*; LBT Type B is also included in comparison. For FixedSD, the self-deferral period is fixed as 10 slot times. Two network deployment scenarios are considered: (1) single-spot deployment (all nodes are placed on the same point, hence there exists no hidden node) and (2) 3GPP indoor scenario [19] as depicted in Fig. 15.

The detailed network configuration is given in the following. The operation frequency band of both networks is the 5 GHz band. Each carrier is 20 MHz wide and the maximum number of carriers that can be aggregated for a data transmission is four. For each node (an eNB/AP and a user device), unless specified otherwise, packet arrivals are generated following the Poisson distribution at a rate of 1000 packets/s for the single-spot scenario and 500 packets/s for the indoor scenario. A wide range of RF leakage bandwidth—the total bandwidth of the adjacent carriers for which the RF leakage power of a carrier exceeds their ED threshold—is considered. In the Wi-Fi network, once a Wi-Fi device (either AP or user station) successfully accesses the medium after backoff, it transmits a data frame with a payload size of 1500 bytes, while an LAA eNB transmits a DL subframe first and a UL subframe transmission immediately follows, each with a length of 1 ms. The transmit power of all node types is 18 dBm. The LBT parameters of LAA follow the 3GPP Technical Specification 36.213 [2]; the slot, defer and short-CCA times—which correspond to the slot, DCF interframe space (DIFS) and PCF interframe space (PIFS) times of Wi-Fi, respectively—are 9, 34 and 25 μs, respectively. The minimum and maximum contention window sizes ($CW_{\min}$ and $CW_{\max}$) are 16 and 1024, respectively, for both networks. The modulation and coding schemes (MCSs) of LAA are QPSK, 16QAM and 64QAM, and those of Wi-Fi include 802.11ac's [56] but 256QAM for fair comparison. The MCS for each user device is selected as the best one based on its channel state information. The ED threshold of LAA is set to -72 dBm while the ED and preamble detection thresholds of Wi-Fi are -62 and -82 dBm, respectively. Estimation of carrier loads (two-tuple information for each carrier) is based on the method of [57] utilizing the CCA results of the latest 3,000 slots (27 ms) and updating the estimated load for each observation of two distinct energy chunks (see Appendix A for the detailed description of the method). The configuration parameters of evaluation are summarized in Table 1.

A. SINGLE-SPOT DEPLOYMENT SCENARIO

In this scenario, the LAA network contains an LAA eNB and ten UEs connected to it, supporting carrier aggregation; the Wi-Fi network has an AP and ten user stations in each carrier.

Fig. 9 shows the LAA system throughput of different LBT options in various RF leakage bandwidth cases. In both DL and UL graphs, Type A - AdaSD shows the best throughput performance among all options in all considered RF leakage

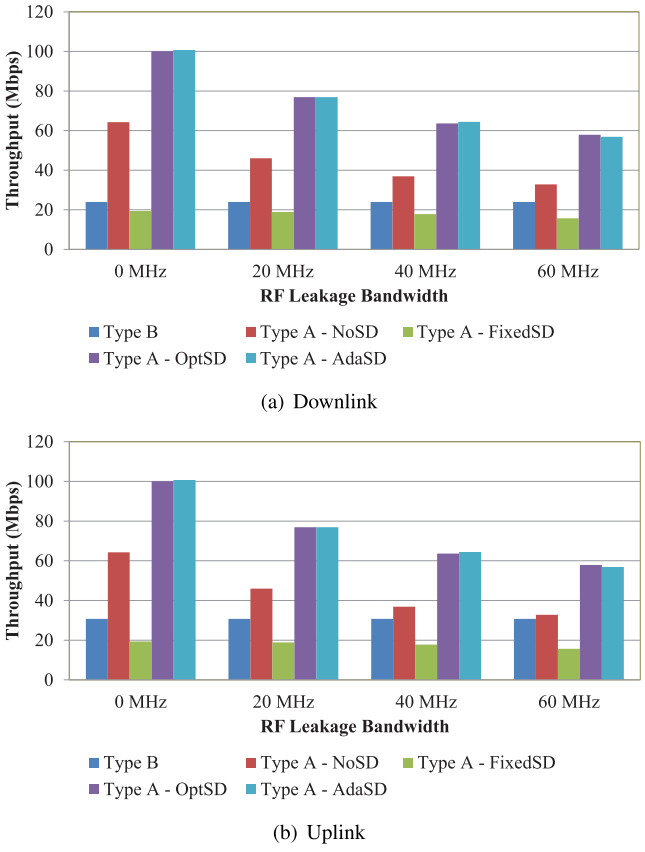

FIGURE 9. DL and UL throughput of LAA with varying RF leakage bandwidth in the single-spot scenario. (a) Downlink. (a) Uplink.

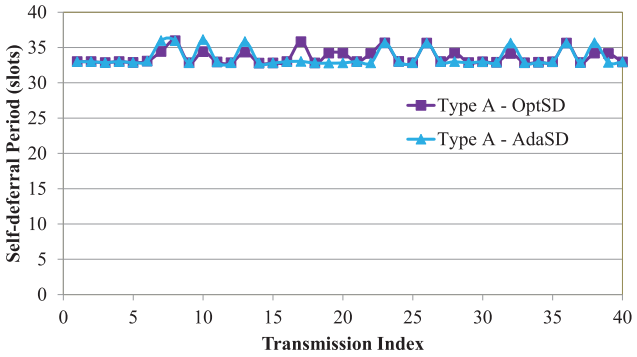

FIGURE 10. Comparison of self-deferral periods between OptSD and AdaSD for example transmissions.

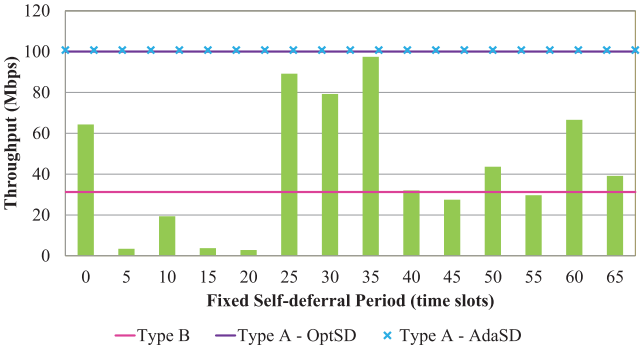

FIGURE 11. DL throughput of LAA for a fixed self-deferral period with various values.

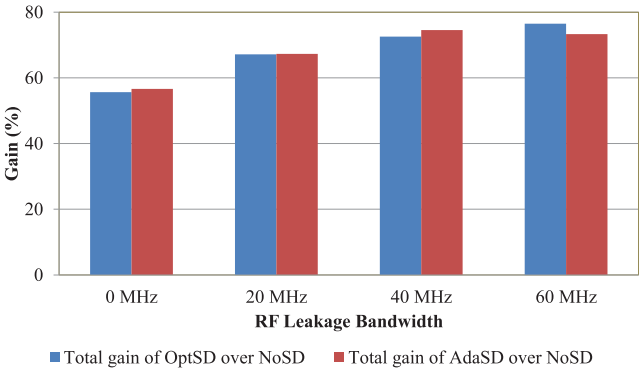

FIGURE 12. Total throughput gain of Type A - OptSD and AdaSD over Type A - NoSD in the single-spot scenario.

cases. It achieves very close to OptSD since AdaSD makes near-optimal determination of the self-deferral period; Fig. 10 compares the self-deferral periods determined by OptSD and AdaSD for a series of transmissions and shows the near-optimality of AdaSD's decisions. It is also noted that AdaSD shows better performance than the others even with no RF leakage. This is because its self-deferral period is determined such that the probability of successful transmission is maximized for each carrier, thus leading to less transmission collisions, which is also effective in single-carrier transmission. Type A - FixedSD has the lowest throughput among all options in all cases, implying that configuration of a proper self-deferral period is of importance, which is also supported by Fig. 11. Type B achieves the second lowest throughput since it is not as efficient as Type A in exploiting multiple carriers.

Type A - NoSD achieves the second best throughput performance in Fig. 9, but, as the RF leakage bandwidth gets wider, the performance gets degraded severer than AdaSD. This is well observed in Fig. 12 where the throughput gain of AdaSD over NoSD increases up to 72% as the RF leakage bandwidth increases; the increasing gain of AdaSD comes from better handling of RF leakage and thus aggregation of more carriers in transmission. For some cases of Fig. 12, AdaSD yields a slightly better throughput than OptSD because of non-perfect estimation of carrier loads; When the estimated load is different from the true one, the self-deferral period chosen by OptSD may not best fit the true load and the choice of AdaSD sometimes happens to be better.

As we show in Fig. 6, the best self-deferral period depends on the current load condition. Therefore, the limitation of using a fixed self-deferral period (FixedSD) is no capability to adapt to changing load conditions, thus not performing well in all cases. Figs. 13 and 14 show this limitation by considering time-changing load conditions (each point of the figures is the average of one second); Wi-Fi's packet generation rate

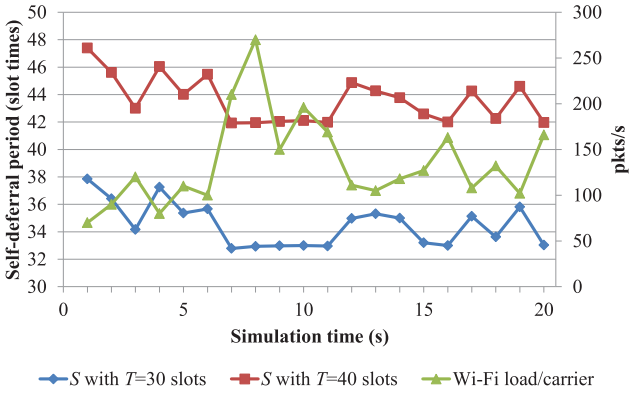

FIGURE 13. Changes of self-deferral period selection under varying Wi-Fi loads.

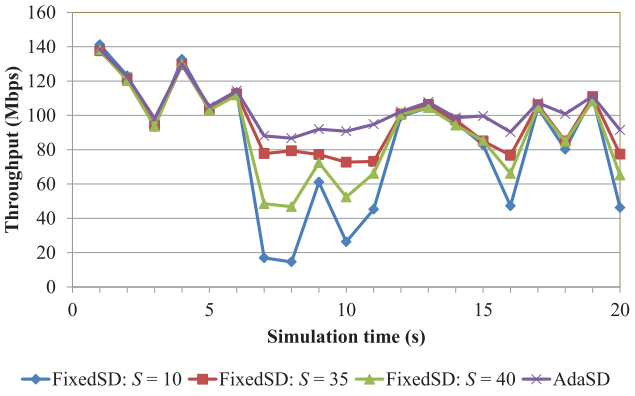

FIGURE 14. Changes of throughput under varying Wi-Fi loads.

changes every second as plotted and two transmission duration (T) cases are considered. As shown in Fig. 13, the self-deferral period chosen by AdaSD changes over time as well. Fig. 14 shows that three FixedSD cases ($S = 10$, 35 and 40) do not always perform well while AdaSD always achieves the best thanks to the adaptation capability of a self-deferral period to changing channel conditions.

B. 3GPP INDOOR DEPLOYMENT SCENARIO

Next, we evaluate the LBT options in the indoor scenario specified in the 3GPP Technical Report 36.889 [19] where each of two operators deploys four cells of either LAA or Wi-Fi in a single-story building as depicted in Fig. 15. Each cell has ten user stations which is randomly distributed around their serving eNB or AP. Since AdaSD is shown to behave similar with OptSD in the previous subsection, OptSD is not included in this simulation.

Fig. 16 shows the average system performance of LAA in the indoor scenario. Similar with the single-spot scenario, AdaSD achieves the best among all options and NoSD is the next. As shown in Fig. 17, the gain of AdaSD over NoSD is maximized as 47% for the RF leakage bandwidth of 60MHz; however, the gains are less than those of the single-spot scenario since the aggregation of carriers is interrupted not only by RF leakage, but also by hidden nodes considerably.

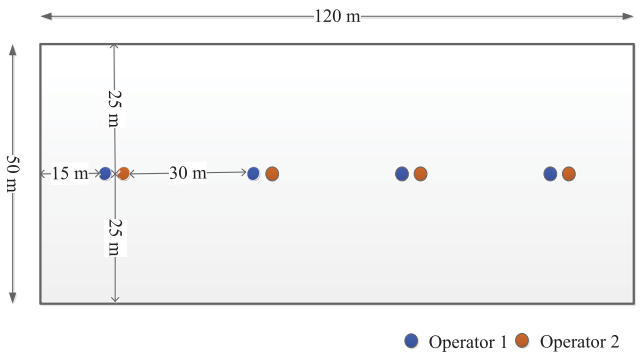

FIGURE 15. 3GPP indoor deployment scenario.

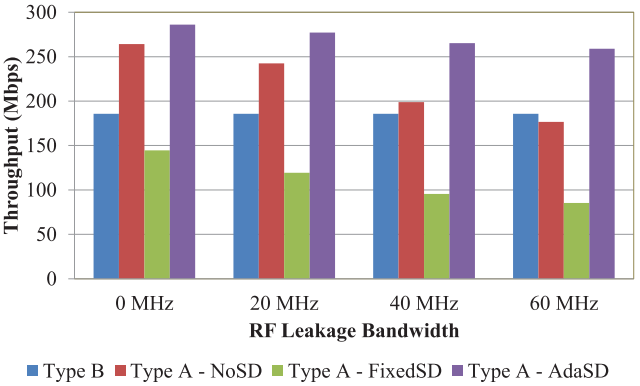

(a) Downlink

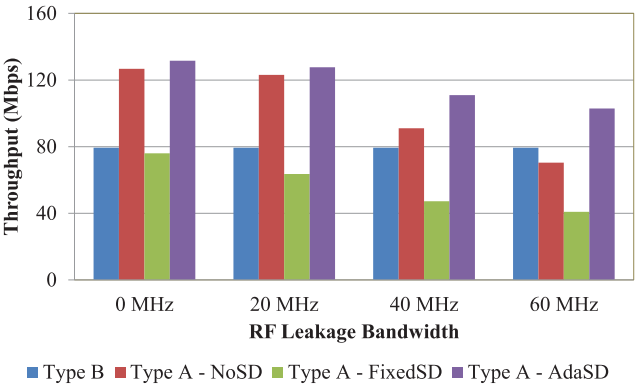

(b) Uplink

FIGURE 16. DL and UL throughput of LAA with varying RF leakage bandwidth in the 3GPP indoor scenario. (a) Downlink. (a) Uplink.

We also present the cumulative distribution functions (CDFs) of per-node (per-eNB/AP for DL and per-user for UL) throughput in Figs. 18 and 19. The CDFs show that AdaSD outperforms the other options not only in the average throughput, but also for most user stations, thus providing enhanced user services.

Fig. 20 shows the average throughput of Wi-Fi for the coexistence cases with different LBT options of LAA. The rightmost bar of each RF leakage bandwidth case is the throughput of Wi-Fi when both operators of the indoor

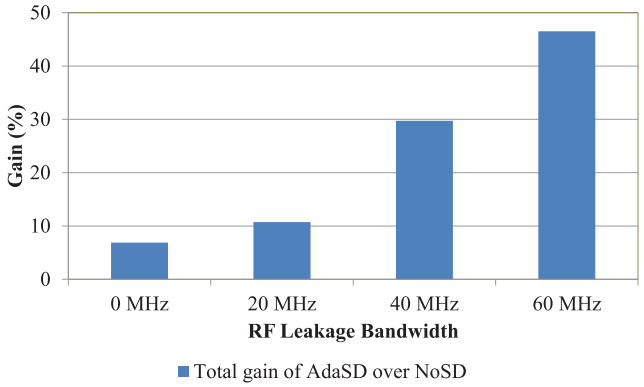

FIGURE 17. Total throughput gain of AdaSD over NoSD in the 3GPP indoor scenario.

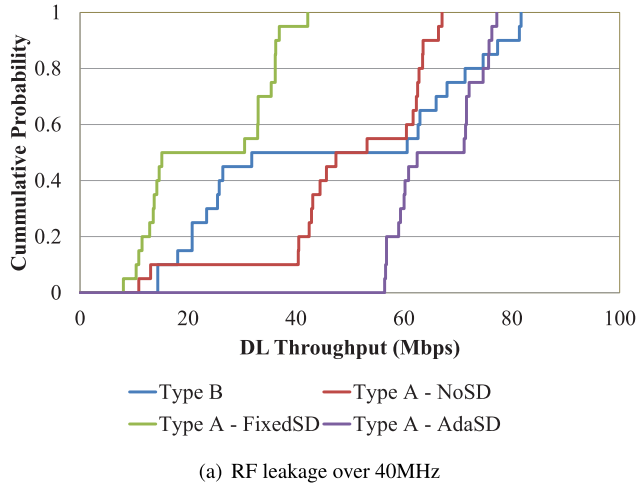

(a) RF leakage over 40MHz

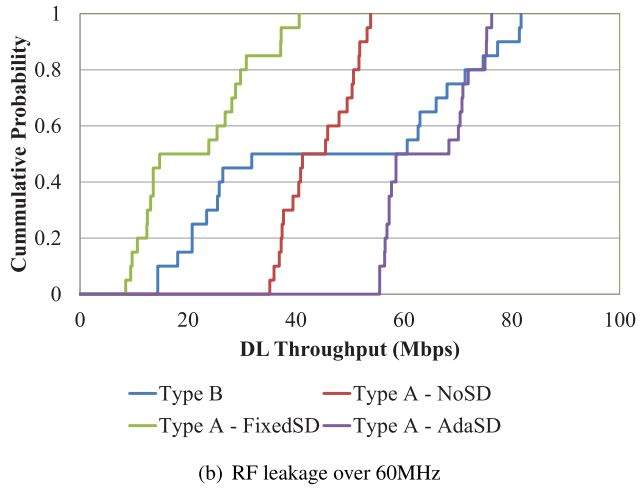

(b) RF leakage over 60MHz

FIGURE 18. CDF of LAA downlink throughput in the 3GPP indoor scenario. (a) RF leakage over 40MHz. (a) RF leakage over 60MHz.

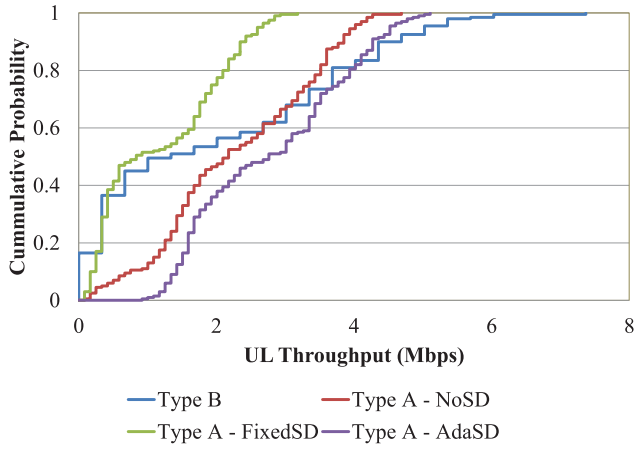

(a) RF leakage over 40MHz

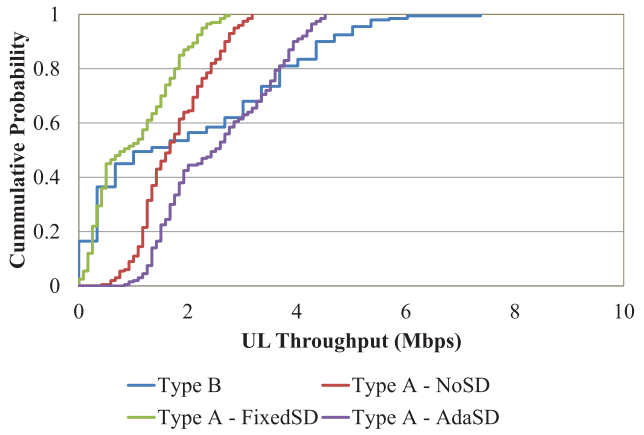

(b) RF leakage over 60MHz

FIGURE 19. CDF of LAA uplink throughput in the 3GPP indoor scenario. (a) RF leakage over 40MHz. (a) RF leakage over 60MHz.

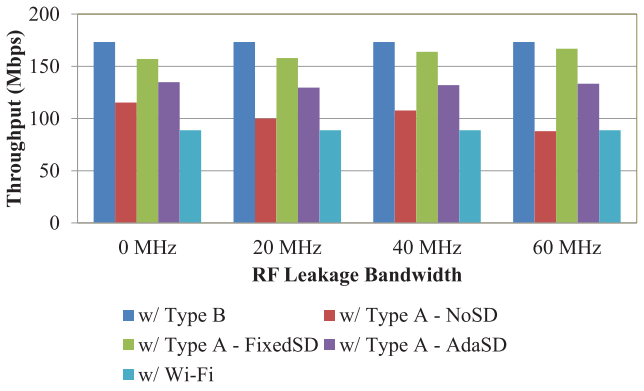

FIGURE 20. Wi-Fi system throughput in the 3GPP indoor scenario.

scenario are Wi-Fi operators, i.e., it is the baseline of coexistence. We then replace one Wi-Fi operator with an LAA operator with various LBT options; if the throughput of Wi-Fi gets worse than the baseline (with a Wi-Fi operator), this means that LAA damages Wi-Fi services and cannot coexist fairly with Wi-Fi systems. The figure shows that the LBT options under consideration do not degrade Wi-Fi performance in the average sense. However, CDFs of Fig. 21(b) show that a significant amount of Wi-Fi users have degraded performance when coexisting with LAA systems of NoSD, implying that the gain of NoSD over FixedSD and Type B

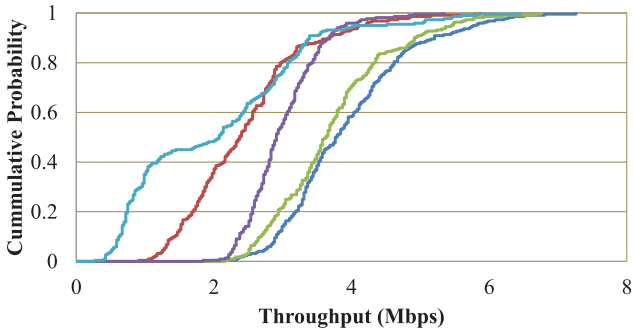

(a) RF leakage over 40MHz

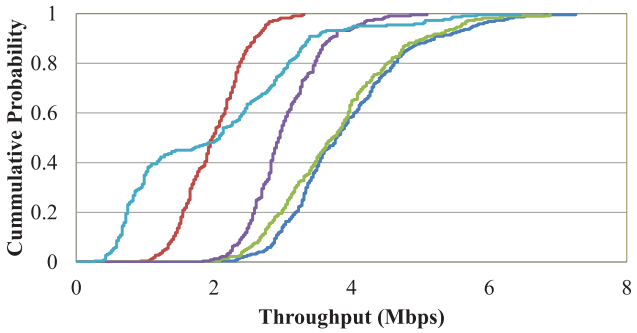

(b) RF leakage over 60MHz

FIGURE 21. CDF of Wi-Fi throughput in the 3GPP indoor scenario. (a) RF leakage over 40MHz. (a) RF leakage over 60MHz.

comes from somewhat aggressive behavior of access on individual carriers.

We also evaluated the computational complexity of Type A - OptSD and AdaSD in terms of the elapsed time of a simulation run, compared with the baseline case of Type A - NoSD. OptSD required 230% additional running time for the single-spot scenario and 156% additional time for the indoor scenario, which shows OptSD to have significant computational overhead. In the meantime, AdaSD took 24% and 11% additional running time, respectively, thus implying that it results in only a marginal increase of computational complexity.

VII. CONCLUSION

We proposed an algorithm to adapt the self-deferral period of an LAA eNB to combat the RF power leakage problem. We formulated the problem of self-deferral as an optimization problem whose objective is to maximize the expected number of aggregated carriers in transmission and derived the optimum for the case of homogeneous interference patterns between carriers. Then, for the case of heterogeneous interference patterns between carriers, the adaptive self-deferral algorithm was designed for configuration of the self-deferral period with low computational complexity. Through extensive simulation, we demonstrated that configuration of the self-deferral period is of importance and the proposed algorithm outperforms various LBT options in a wide range of network configuration and deployment scenarios while meeting fair coexistence with Wi-Fi systems.

APPENDIX. CARRIER LOAD ESTIMATION

In the channel-usage model of [57], the transmission activity of a carrier is modeled as alternating ON (busy) and OFF (idle) periods based on the theory of alternating renewal process. The durations of ON and OFF periods are modeled as independent random variables T_{ON} and T_{OFF}, respectively. The model further assumes that ON and OFF periods are independent and identically distributed (i.i.d). Previous research works showed that the MAC service time of IEEE 802.11 is well approximated by the exponential distribution (or its discrete analogue, geometric distribution) [58], [59]. Therefore, if we assume that the transmission duration of IEEE 802.11 follows the exponential distribution, we can approximate ON and OFF periods as exponentially-distributed random variables. Then, the parameters to identify the model are the means of the two random variables, which we denote by $1/\lambda_{T_{ON}}$ and $1/\lambda_{T_{OFF}}$, respectively, for ON and OFF periods.

Ideally, if the model parameters are known accurately, the two-tuple information of the load condition of a carrier, p and T, is obtained as

$$\begin{aligned} p &= u - u \cdot e^{-(\lambda_{T_{OFF}} + \lambda_{T_{ON}})T_{sl}}, \\ T &= E[T_{ON}] = 1/\lambda_{T_{ON}} \end{aligned} \tag{13}$$

where u is defined as the channel utilization and given as

$$\begin{aligned} u &= E[T_{ON}]/(E[T_{ON}] + E[T_{OFF}]) \\ &= \lambda_{T_{OFF}}/(\lambda_{T_{OFF}} + \lambda_{T_{ON}}). \end{aligned} \tag{14}$$

However, in reality, these model parameters are not known a priori and even change over time. So, we let an LAA eNB estimate the load condition of each carrier from r number of latest CCA results, denoted by $(Z_{t_1}, Z_{t_2}, \ldots, Z_{t_r})$ where $Z_{t_k} \in \{0, 1\}$ is the result of CCA at time t_k (0 denotes idle and 1 denotes busy). These r CCA results lead to $r - 1$ pairs of consecutive results; we denote the numbers of such pairs for $(0 \rightarrow 0)$ and $(1 \rightarrow 1)$ by $n_{0,0}$ and $n_{1,1}$, respectively. We denote the estimated versions of the model parameters by putting a hat on each, i.e., $\hat{\lambda}_{T_{ON}}$, $\hat{\lambda}_{T_{OFF}}$ and $\hat{u}$.

From [57], $\hat{u}$ and $\hat{\lambda}_{T_{OFF}}$ are given as

$$\begin{aligned} \hat{u} &= \frac{1}{r}\sum_{k=1}^{r} Z_{t_k}, \\ \hat{\lambda}_{T_{OFF}} &= -\frac{\hat{u}}{T_{sl}} \ln\left[\frac{-B + \sqrt{B^2 - 4AC}}{2A}\right] \end{aligned} \tag{15}$$

where

$$A = (\hat{u} - \hat{u}^2)(r-1),$$
$$B = -2A + (r-1) - (1-\hat{u})n_{0,0} - \hat{u} \cdot n_{1,1},$$
$$C = A - \hat{u} \cdot n_{0,0} - (1-\hat{u})n_{1,1}. \quad (16)$$

Applying (15) into (14), we obtain $\hat{\lambda}_{T_{ON}}$ as

$$\hat{\lambda}_{T_{ON}} = \frac{(1-\hat{u})\hat{\lambda}_{T_{OFF}}}{\hat{u}}. \quad (17)$$

Finally, using the estimated model parameters of (15) and (17) in (13), we obtain the estimated versions of p and T for the carrier.

REFERENCES

[1] *Evolved Universal Terrestrial Radio Access (E-UTRA); Overall Description*, document TS 36.300, 3GPP, Rev. 15.4.0, Jan. 2019.
[2] *Evolved Universal Terrestrial Radio Access (E-UTRA); Physical Layer Procedures*, document TS 36.213, 3GPP, Rev. 15.4.0, Jan. 2019.
[3] *Evolved Universal Terrestrial Radio Access (E-UTRA); Base Station (BS) Radio Transmission and Reception*, document TS 36.104, 3GPP, Rev. 16.0.0, Jan. 2019.
[4] *Multi-Carrier LBT Operation for LAA*, document R1-152784, 3GPP, Qualcomm, Oct. 2015.
[5] H. Zhang, X. Chu, W. Guo, and S. Wang, "Coexistence of Wi-Fi and heterogeneous small cell networks sharing unlicensed spectrum," *IEEE Commun. Mag.*, vol. 53, no. 3, pp. 158–164, Mar. 2015.
[6] E. Almeida, A. M. Cavalcante, R. C. D. Paiva, F. S. Chaves, F. M. Abinader, R. D. Vieira, S. Choudhury, E. Tuomaala, and K. Doppler, "Enabling LTE/WiFi coexistence by LTE blank subframe allocation," in *Proc. IEEE ICCW*, Jun. 2013, pp. 5083–5088.
[7] T. Nihtilä, V. Tykhomyrov, O. Alanen, M. A. Uusitalo, A. Sorri, M. Moisio, S. Iraji, R. Ratasuk, and N. Mangalvedhe, "System performance of LTE and IEEE 802.11 coexisting on a shared frequency band," in *Proc. IEEE WCNC*, Apr. 2013, pp. 1038–1043.
[8] F. M. Abinader, E. P. L. Almeida, F. S. Chaves, A. M. Cavalcante, R. D. Vieira, R. C. D. Paiva, A. M. Sobrinho, S. Choudhury, E. Tuomaala, K. Doppler, and V. A. Sousa, "Enabling the coexistence of LTE and Wi-Fi in unlicensed bands," *IEEE Commun. Mag.*, vol. 52, no. 11, pp. 54–61, Nov. 2014.
[9] N. Rupasinghe and I. Güvenç, "Reinforcement learning for licensed-assisted access of LTE in the unlicensed spectrum," in *Proc. IEEE Wireless Commun. Netw. Conf. (WCNC)*, Mar. 2015, pp. 1279–1284.
[10] S. Han, Y.-C. Liang, Q. Chen, and B.-H. Soong, "Licensed-assisted access for LTE in unlicensed spectrum: A MAC protocol design," *IEEE J. Sel. Areas Commun.*, vol. 34, no. 10, pp. 2550–2561, Oct. 2016.
[11] C. Cano and D. J. Leith, "Coexistence of WiFi and LTE in unlicensed bands: A proportional fair allocation scheme," in *Proc. IEEE Int. Conf. Commun. Workshop (ICCW)*, London, U.K., Jun. 2015, pp. 2288–2293.
[12] R. Zhang, M. Wang, L. X. Cai, X. Shen, L.-L. Xie, and Y. Cheng, "Modeling and analysis of MAC protocol for LTE-U co-existing with Wi-Fi," in *Proc. IEEE GLOBECOM*, Dec. 2015, pp. 1–6.
[13] Y. Li, F. Baccelli, J. G. Andrews, T. D. Novlan, and J. C. Zhang, "Modeling and analyzing the coexistence of Wi-Fi and LTE in unlicensed spectrum," *IEEE Trans. Wireless Commun.*, vol. 15, no. 9, pp. 6310–6326, Sep. 2016.
[14] M. Maule, D. Moltchanov, P. Kustarev, M. Komarov, S. Andreev, and Y. Koucheryavy, "Delivering fairness and QoS guarantees for LTE/Wi-Fi coexistence under LAA operation," *IEEE Access*, vol. 6, pp. 7359–7373, 2018.
[15] B. C. Chung and D.-H. Cho, "Mobile data offloading with almost blank subframe in LTE-LAA and Wi-Fi coexisting networks based on coalition game," *IEEE Commun. Lett.*, vol. 21, no. 3, pp. 608–611, Mar. 2017.
[16] C. Cano, D. J. Leith, A. Garcia-Saavedra, and P. Serrano, "Fair coexistence of scheduled and random access wireless networks: Unlicensed LTE/WiFi," *IEEE/ACM Trans. Netw.*, vol. 25, no. 6, pp. 3267–3281, Dec. 2017.
[17] A.-K. Ajami and H. Artail, "On the modeling and analysis of uplink and downlink IEEE 802.11ax Wi-Fi with LTE in unlicensed spectrum," *IEEE Trans. Wireless Commun.*, vol. 16, no. 9, pp. 5779–5795, Sep. 2017.
[18] Z. Guan and T. Melodia, "CU-LTE: Spectrally-efficient and fair coexistence between LTE and Wi-Fi in unlicensed bands," in *Proc. IEEE INFOCOM*, Apr. 2016, pp. 1–9.
[19] *Feasibility Study on Licensed-Assisted Access to Unlicensed Spectrum*, document TR 36.889, 3GPP, Rev. 13.0.0, Jul. 2015.
[20] B. Jia and M. Tao, "A channel sensing based design for LTE in unlicensed bands," in *Proc. IEEE ICCW*, Jun. 2015, pp. 2332–2337.
[21] C. Casetti, "Coexistence of IEEE 802.11n and licensed-assisted access devices using listen-before-talk techniques," in *Proc. IEEE CCNC*, Jan. 2016, pp. 562–567.
[22] C. Chen, R. Ratasuk, and A. Ghosh, "Downlink performance analysis of LTE and WiFi coexistence in unlicensed bands with a simple listen-before-talk scheme," in *Proc. IEEE VTC*, May 2015, pp. 1–5.
[23] A. Mukherjee, J.-F. Cheng, S. Falahati, L. Falconetti, A. Furuskär, B. Godana, D. H. Kang, H. Koorapaty, D. Larsson, and Y. Yang, "System architecture and coexistence evaluation of licensed-assisted access LTE with IEEE 802.11," in *Proc. IEEE ICCW*, Jun. 2015, pp. 2350–2355.
[24] A. V. Kini, L. Canonne-Velasquez, M. Hosseinian, M. Rudolf, and J. Stern-Berkowitz, "Wi-Fi-LAA coexistence: Design and evaluation of listen before talk for LAA," in *Proc. Annu. Conf. Inf. Sci. Syst. (CISS)*, Mar. 2016, pp. 157–162.
[25] L. Li, J. P. Seymour, L. J. Cimini, and C.-C. Shen, "Coexistence of Wi-Fi and LAA networks with adaptive energy detection," *IEEE Trans. Veh. Technol.*, vol. 66, no. 11, pp. 10384–10393, Nov. 2017.
[26] S. Xu, Y. Li, Y. Gao, Y. Liu, and H. Gačanin, "Opportunistic coexistence of LTE and WiFi for future 5G system: Experimental performance evaluation and analysis," *IEEE Access*, vol. 6, pp. 8725–8741, 2018.
[27] H. Lee, H. Kim, H. J. Yang, J. T. Kim, and S. Baek, "Performance analysis of license assisted access LTE with asymmetric hidden terminals," *IEEE Trans. Mobile Comput.*, vol. 17, no. 9, pp. 2141–2154, Sep. 2018.
[28] Y. Li, T. Zhou, Y. Yang, H. Hu, and M. Hamalainen, "Fair downlink traffic management for hybrid LAA-LTE/Wi-Fi networks," *IEEE Access*, vol. 5, pp. 7031–7041, 2017.
[29] T. Tao, F. Han, and Y. Liu, "Enhanced LBT algorithm for LTE-LAA in unlicensed band," in *Proc. IEEE PIMRC*, Aug./Sep. 2015, pp. 1907–1911.
[30] R. Yin, G. Yu, A. Maaref, and G. Y. Li, "Adaptive LBT for licensed assisted access LTE networks," in *Proc. IEEE GLOBECOM*, Dec. 2015, pp. 1–6.
[31] K. Yoon, T. Park, J. Kim, W. Sun, S. Hwang, I. Kang, and S. Choi, "COTA: Channel occupancy time adaptation for LTE in unlicensed spectrum," in *Proc. IEEE DySPAN*, Mar. 2017, pp. 1–10.
[32] O. Sallent, J. Pérez-Romero, R. Ferrús, and R. Agustí, "Learning-based coexistence for LTE operation in unlicensed bands," in *Proc. IEEE ICCW*, Jun. 2015, pp. 2307–2313.
[33] S. Sagari, S. Baysting, D. Saha, I. Seskar, W. Trappe, and D. Raychaudhuri, "Coordinated dynamic spectrum management of LTE-U and Wi-Fi networks," in *Proc. IEEE DySPAN*, Sep. 2015, pp. 209–220.
[34] S.-Y. Lien, J. Lee, and Y.-C. Liang, "Random access or scheduling: Optimum LTE licensed-assisted access to unlicensed spectrum," *IEEE Commun. Lett.*, vol. 20, no. 3, pp. 590–593, Mar. 2016.
[35] C. G. Tsinos, F. Foukalas, and T. A. Tsiftsis, "Resource allocation for licensed/unlicensed carrier aggregation MIMO systems," *IEEE Trans. Commun.*, vol. 65, no. 9, pp. 3765–3779, Sep. 2017.
[36] Y. Gu, Y. Wang, and Q. Cui, "A stochastic optimization framework for adaptive spectrum access and power allocation in licensed-assisted access networks," *IEEE Access*, vol. 5, pp. 16484–16494, 2017.
[37] H. Zhang, Y. Xiao, L. X. Cai, D. Niyato, L. Song, and Z. Han, "A hierarchical game approach for multi-operator spectrum sharing in LTE unlicensed," in *Proc. IEEE GLOBECOM*, Dec. 2015, pp. 1–6.
[38] Y. Gu, Y. Zhang, L. Cai, M. Pan, L. Song, and Z. Han, "LTE-unlicensed coexistence mechanism: A matching game framework," *IEEE Wireless Commun. Mag.*, vol. 23, no. 6, pp. 54–60, Dec. 2016.
[39] Q. Chen, G. Yu, A. Maaref, G. Y. Li, and A. Huang, "Rethinking mobile data offloading for LTE in unlicensed spectrum," *IEEE Trans. Wireless Commun.*, vol. 15, no. 7, pp. 4987–5000, Jul. 2016.
[40] *Way Forward LBT for Multi-Carrier Transmission in LAA DL*, document R1-153548, 3GPP, Qualcomm, Huawei, Hisilicon, May 2015.
[41] *Multi-Carrier LBT Design and Performance Evaluation for LAA DL*, document R1-154079, 3GPP, Intel, Aug. 2015.
[42] *LAA Multi-Channel LBT*, document R1-155458, 3GPP, Samsung, Oct. 2015.
[43] *Discussion Wi-Fi and DL-Only LAA Coexistence for Multi-Channel Transmission*, document R1-154624, 3GPP, Ericsson, Aug. 2015.
[44] *Discussion LAA DL Multi-Carrier LBT*, document R1-155547, 3GPP, Broadcom, Oct. 2015.

[45] *Multi-Carrier LBT Operation for LAA*, document R1-155816, 3GPP, Lenovo, Oct. 2015.
[46] *Discussion Multi-Carrier LBT for LAA*, document R1-155940, 3GPP, WILUS, Oct. 2015.
[47] *On Channel Access Solutions for LAA Multi-Carrier Transmission*, document R1-156033, 3GPP, Ericsson, Oct. 2015.
[48] *Consideration Multi-Carrier LBT for LAA*, 3GPP, document R1-157330, WILUS, Nov. 2015.
[49] J. Liu and G. Shen, "Performance of multi-carrier LBT mechanism for LTE-LAA," in *Proc. IEEE VTC*, May 2016, pp. 1–5.
[50] S. Wang, Q. Cui, and Y. Gu, "Performance analysis of multi-carrier LAA and Wi-Fi coexistence in unlicensed spectrum," in *Proc. IEEE ICCC*, Oct. 2017, pp. 1–5.
[51] L. H. Vu and J.-H. Yun, "Power leakage-aware multi-carrier LBT for LTE-LAA in unlicensed spectrum," in *Proc. IEEE DySPAN*, Oct. 2018, pp. 211–220.
[52] *LTE in Unlicensed Spectrum: Harmonious Coexistence with Wi-Fi*, Qualcomm Technol., San Diego, CA, USA, Jun. 2014.
[53] S. Boyd and L. Vandenberghe, *Convex Optimization*. Cambridge, U.K.: Cambridge Univ. Press, 2004.
[54] J. A. Nelder and R. Mead, "A simplex method for function minimization," *Comput. J.*, vol. 7, no. 4, pp. 308–313, 1965.
[55] Microsoft. (2011). *Microsoft Solver Foundation 3.1*. [Online]. Available: https://docs.microsoft.com/en-us/previous-versions/visualstudio/ff524509(v=vs.93)
[56] *Wireless LAN Medium Access Control (MAC) Physical Layer (PHY) Specifications*, IEEE Standard 802.11, 2016.
[57] H. Kim and K. G. Shin, "Efficient discovery of spectrum opportunities with MAC-layer sensing in cognitive radio networks," *IEEE Trans. Mobile Comput.*, vol. 7, no. 5, pp. 533–545, May 2008.
[58] X. Chen, H. Zhai, X. Tian, and Y. Fang, "Supporting QoS in IEEE 802.11e wireless LANs," *IEEE Trans. Wireless Commun.*, vol. 5, no. 8, pp. 2217–2227, Aug. 2006.
[59] A. Abdrabou and W. Zhuang, " Service time approximation in IEEE 802.11 single-hop ad hoc networks," *IEEE Trans. Wireless Commun.*, vol. 7, no. 1, pp. 305–313, Jan. 2008.

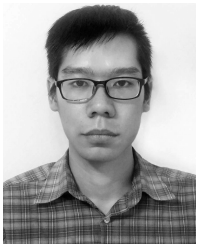

LONG HOANG VU received the B.S. degree in electronics and telecommunications engineering from the Hanoi University of Science and Technology (HUST), Hanoi, Vietnam, in 2012, and the M.S. degree in electrical and information engineering from the Seoul National University of Science and Technology (SeoulTech), Seoul, South Korea, in 2015, where he is currently pursuing the Ph.D. degree in electrical and information engineering. His current research focuses on cellular communications in unlicensed spectrum.

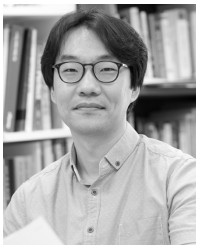

JI-HOON YUN received the B.S. degree in electrical engineering from Seoul National University (SNU), Seoul, South Korea, in 2000, and the M.S. and Ph.D. degrees in electrical engineering and computer science from SNU, in 2002 and 2007, respectively.

He is currently an Associate Professor with the Department of Electrical and Information Engineering, Seoul National University of Science and Technology (SeoulTech), Seoul, South Korea. Before joining SeoulTech, in 2012, he was with the Department of Computer Software Engineering, Kumoh National Institute of Technology, as an Assistant Professor. He was a Postdoctoral Researcher with the Real-Time Computing Laboratory, The University of Michigan, Ann Arbor, MI, USA, in 2010, and a Senior Engineer with the Telecommunication Systems Division, Samsung Electronics, Suwon, South Korea, from 2007 to 2009. His current research focuses on mobile networking and computing.